CHAPTER TWENTY-ONE

Visualizing Yeast Chromosomes and Nuclear Architecture

Peter Meister, Lutz R. Gehlen, Elisa Varela,[1] Véronique Kalck, *and* Susan M. Gasser

Contents

Abstract

We describe here optimized protocols for tagging genomic DNA sequences with bacterial operator sites to enable visualization of specific loci in living budding yeast cells. Quantitative methods for the analysis of locus position relative to the nuclear center or nuclear pores, the analysis of chromatin dynamics and the relative position of tagged loci to other nuclear landmarks are described.

Friedrich Miescher Institute for Biomedical Research, Basel, Switzerland
[1] Present address: Fundacion Centro Nacional de Investigaciones Oncologicas Carlos IIII, Melchor Fernandez Almagro 3, Madrid, Spain

Methods in Enzymology, Volume 470
ISSN 0076-6879, DOI: 10.1016/S0076-6879(10)70021-5

Methods for accurate immunolocalization of nuclear proteins without loss of three-dimensional structure, in combination with fluorescence *in situ* hybridization, are also presented. These methods allow a robust analysis of subnuclear organization of both proteins and DNA in intact yeast cells.

1. Introduction

Quantitative imaging techniques have improved dramatically in the last 15 years, reflecting both the rapid adaptation of naturally fluorescent proteins to cellular applications and improvements in fluorescence microscopy itself. Methods are also being continually optimized for the analysis and localization of endogenous proteins and chromosomal loci in living yeast cells. This involves novel microscope systems as well as improved computational tools for image analysis. Crucial to this process are tools for the rapid processing of the high-resolution digital-image stacks, since megabytes of data are produced in a single 3D time-lapse experiment on either a deconvolution widefield microscope or spinning disk (SD) confocal instrument (Hom *et al.*, 2007).

While techniques of live microscopy are powerful, it is not trivial to perform them correctly. Specifically, accurate visualization of more than two fluorophores at the same time can be difficult, and care must be taken to avoid damage by the light that is used for imaging. This can be particularly problematic when dealing with mutants that enhance sensitivity to damage or stress. Maintenance of unperturbed growth conditions and minimization of exposure time and light intensity are essential for meaningful results. Because high-resolution time-lapse microscopy often captures only one or a few cells per 3D stack, the imaging step can itself take considerable time, rendering it difficult to obtain sufficient numbers of cells or to carry out large time-course experiments. If several strains are to be analyzed in parallel, it is recommended that cells be fixed by formaldehyde at the desired time points, so that the localization of proteins or DNA can be achieved later by immunofluorescence (IF) and/or fluorescent probe *in situ* hybridization (FISH).

This chapter contains two sets of optimized protocols for the visualization of specific proteins and/or DNA sequences in budding yeast. The first set describes the targeting and analysis of proteins fused to the fluorescent protein GFP or its derivatives. The second section describes more classical methods for IF and/or FISH, which are sometimes the methods of choice for visualizing different types of macromolecules at once. Basic methods for quantitative analysis of subnuclear position and chromatin dynamics are described. These methods have been optimized for the localization of one or several targets in the nucleus relative to DNA or the nuclear envelope (NE). We note that improvements are continually being made in these procedures and that future users should seek updates on the methodology in the literature.

2. Strain Constructions and Image Acquisition for Nuclear Architecture Analysis in Living Cells

2.1. Tagging chromatin *in vivo* with *lac* and *tet* operator arrays

The study of chromatin organization in live budding yeast cells often exploits the recognition of integrated arrays by fluorescently labeled bacterial DNA binding factors, usually the LacI or TetR repressor (reviewed in Belmont, 2001; Hediger *et al.*, 2004; Neumann *et al.*, 2006). The target arrays consist of anywhere from 100 to 256 copies of the recognition consenses (*lacO* or *tetO*). As few as 24 binding sites are usually sufficient to allow the formation of a visible spot, although the signal-to-noise ratio depends on the expression level of the fluorescently tagged binding protein.

Tagging chromatin *in vivo* is a two-step process. The first step involves the expression of a fusion between a DNA-binding protein, a fluorescent protein, and a nuclear localization signal. Both integrative and episomal plasmids have been used to express these proteins (Michaelis *et al.*, 1997; Straight *et al.*, 1996). Integrative plasmids give more reproducible levels of the fluorescently tagged proteins. The DNA binding Lac repressor is expressed as a fusion with green fluorescent protein (GFP), the cyan and/or yellow variants (CFP, YFP), and the Tet repressor exists as fusion proteins with GFP, CFP, YFP, and the monomeric variant of the red fluorescent protein, mRFP (Lisby *et al.*, 2003). To increase the fluorescence signal, a fluorescent protein can be introduced as a tandem array (3× CFP, Bressan *et al.*, 2004). Expression levels of these proteins have to be kept low, as overexpression elevates the background fluorescence, enhances non-specific binding, and can cause slow growth.

The binding site arrays recognized by the fluorescently labeled repressors are repetitive and unstable by nature in both bacteria and yeast. To avoid recombination and loss of copy number, the bacteria (either DH5α or recombination-deficient strains like SURE (Stratagene)) should be grown at 25 or 30 °C. When thawing bacterial strains, several colonies have to be tested for the size of the array by digestion of plasmid preparations with enzymes encompassing the array. The binding sites are inserted as an array in strains expressing the fluorescent DNA-binding proteins. For unknown reasons, expression of the DNA-binding protein in yeast stabilizes the array; therefore, it is recommended to transform yeast with the fusion protein construct prior to introducing the *lacO* or *tetO* sites.

To date, three techniques have been used to insert arrays at specific loci in the yeast genome. The first technique is based on the cloning of a small PCR-generated fragment of genomic DNA (about 400–800 bp) into the array-containing plasmid (Fig. 21.1A, Heun *et al.*, 2001a,b). This fragment

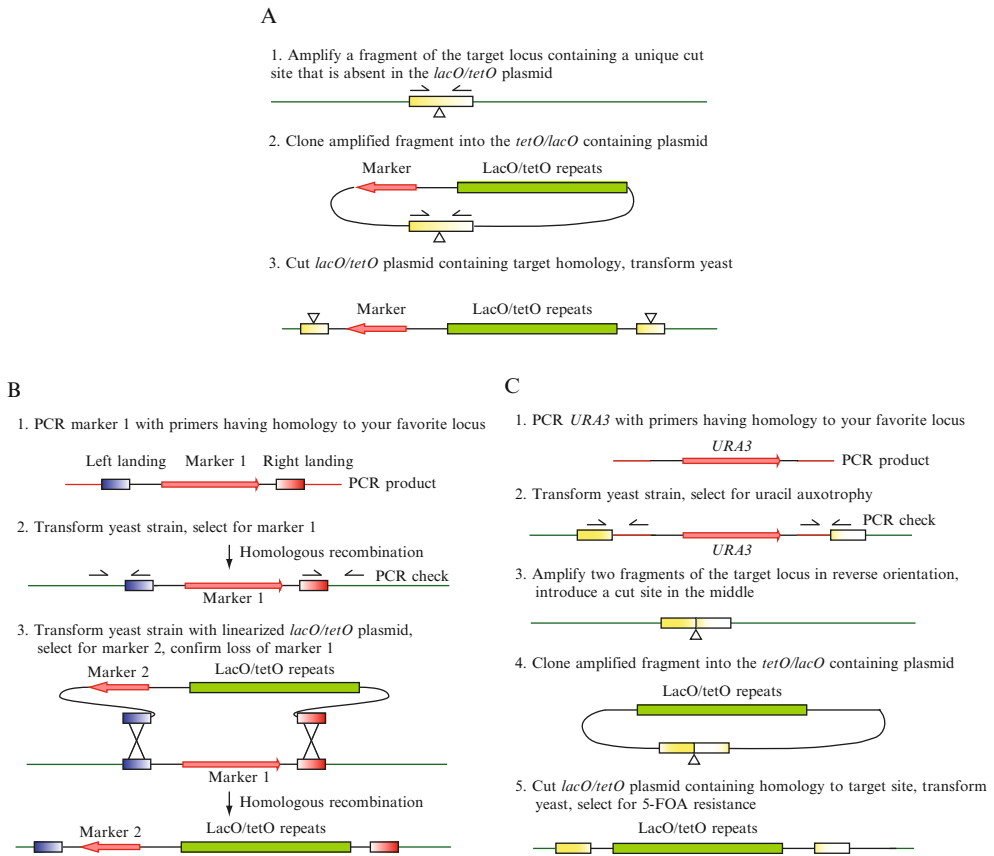

Figure 21.1 Outline of the methods for site-specific integration of *lacO/tetO* repeats in the genome cloning-free chromatin tagging. For details see text.

is chosen so that it contains a unique restriction site that is not present in the *lacO/tetO* plasmid. Once cloned into the array, digestion with this single-cutter enzyme will linearize the plasmid, which can be used for homologous recombination. The homology created by the small genome segment targets the plasmid to the desired genomic locus. It also creates direct repeats flanking the array, which might be detrimental to the stability of the array, as these allow popping-out of the whole plasmid by recombination between the two direct repeats. Positive transformants are selected by resistance to a selective marker present on the plasmid then correct insertion is tested by PCR and/or southern blotting. During the transformation process, some binding site repeats may be lost, therefore transformed yeast colonies have to be screened microscopically for the presence of a bright spot. One should not store the resulting yeast strains at room temperature for more than a week and positive clones should be frozen immediately. Spot presence has to be reconfirmed after thawing.

The second technique was developed to avoid tedious cloning steps with large plasmids containing *lacO/tetO* repeats (Rohner *et al.*, 2008). It is a two-step process involving first PCR-based integration of a marker flanked by 100-bp tags at the locus of interest. Once the tags are integrated into the genome at the locus of interest, they can be used for homologous recombination to integrate *lacO/lexA* repeats and a second selectable marker (Fig. 21.1B). To this end, the tags are cloned into the *lacO/tetO* repeat plasmid in reverse orientation with a rare cutting site in between them. When cut with this enzyme, the two adaptamers encompass the *lacO/tetO* repeats and can therefore be aligned with the tags flanking the marker in the genome. This technique is more flexible in terms of markers and allows one to tag the same locus with different binding sites without the need to reclone a PCR fragment into an array-containing plasmid.

A third technique combines the previous two and has been developed to avoid integrating a marker gene next to the repeats (Fig. 21.1C; Kitamura *et al.*, 2006). In a first step, a *URA3* gene is inserted at the locus of interest using long primer PCR-mediated recombination. To achieve replacement of the *URA3* gene, a fragment of about 700 bp corresponding to the *URA3* insertion site is cloned in the *lacO/tetO* repeat plasmid. As for the first technique described above, the recipient plasmid contains a single cut site in the middle of the cloned fragment. Transformation of the cut plasmid leads to replacement of *URA3* by the repeats. In this case, positive colonies are selected by their ability to grow on 5-fluoro-orotic acid (FOA), which is toxic in the presence of *URA3*. The main drawback of this technique is that it does not allow selection of the colonies which still contain the array, for example, after freezing. Direct replacement of *URA3* using an adaptamer-based technique with a marker-free plasmid is impossible, as FOA-resistant colonies arise more frequently than recombination events.

It is often useful to insert a low number of binding sites for another DNA-binding protein next to the *lacO* or *tetO* sites integrated at specific loci. This allows one to target another protein to the site of interest, which can be used to manipulate the locus. For example, integrated lexA sites allow binding of lexA fusion proteins, such as a lexA–Yif1 fusion, that anchors the tagged chromatin locus to the NE (Taddei *et al.*, 2004). Plasmids for the tagging methods described above are available with lexA binding sites located next to the *lacO*/*tetO* repeats (Rohner *et al.*, 2008; Taddei *et al.*, 2004). Other locus-tagging systems in development include a lambda repressor/operator system (K. Bystricky, A. Taddei, personal communication).

2.2. Determining the position of the nucleus

For precise localization studies, as well as for studying chromatin dynamics, the nuclear volume has to be defined. This can be achieved either by expression of a nucleoporin fused to a fluorescent protein (commonly Nup49-GFP) or by using the nuclear background fluorescence created by the unbound TetR protein. LacI-GFP tends to give very little background even in the absence of a *lacO* array, probably due to its low expression level.

2.3. Immobilizing cells for microscopy

To obtain images which allow the reliable measurement of chromatin position and dynamics there are two central concerns. First, one must immobilize the yeast cells and second one must prevent distortion of cell shape by pressure from the coverslip or objective. Both are achieved by the following methods.

For "snapshot" exposures where yeasts will be imaged only once, living cells are mounted on pad of agarose in synthetic medium. Immobilizing cells between agarose and a coverslip does not flatten or distort cells, while coverslip pressure on a glass slide does. Optimal agarose patches are created on depression slides, which have a concave depression in which the agarose and cells are placed. The agarose (1.4%) is dissolved in an appropriate medium (YPD gives more background than SD), and if imaging or cell maintenance lasts more than 20–30 min, it is recommended to use higher than usual levels of glucose (4% instead of 2%). Glucose can be locally depleted by cells in the agarose pad, while they are being imaged, and this reduces chromatin mobility within nuclei (Heun *et al.*, 2001b). Agarose prepared with yeast medium can be distributed in aliquots and kept for months at room temperature.

1. Prior to use, agarose is dissolved in growth media at 95 °C for several minutes. The agarose should be liquid, but prolonged maintenance at high temperature increases background fluorescence.

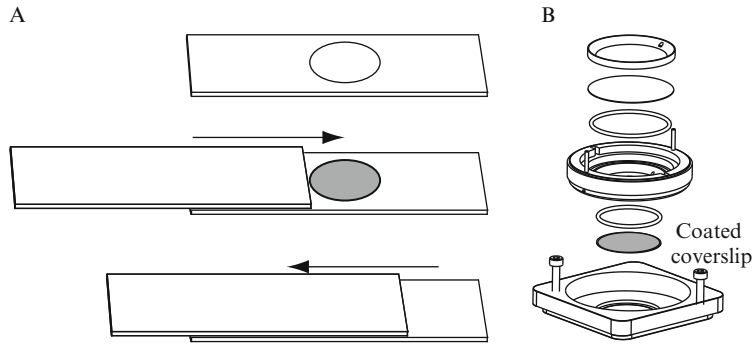

Figure 21.2 Means to immobilize yeast cells for imaging. (A) Formation of a flat-topped pad of agarose dissolved in media on a depression slide. (B) Cell observation chamber (Ludin chamber, Life Imaging Services) with cells immobilized on the lectin-coated bottom glass coverslide is shown.

2. Melted agarose is then poured into the depression of the slide.
3. A normal slide is immediately placed across the top to remove excess agarose and create a flat surface on the pad (Fig. 21.2A). While the agarose solidifies, 1 ml of an exponentially growing culture (at concentrations $< 0.5 \times 10^7$ cells/ml) is spun in a microcentrifuge and resuspended in 20 μl of appropriate medium. Cells can be grown in synthetic medium or YPD, but YPD cultures show more autofluorescence. Note that high cell density or glucose depletion alter chromatin dynamics (Heun *et al.*, 2001b).
4. After removal of the upper slide by sliding along the depression slide surface, 5 μl of the concentrated cells are placed on the agarose, and the pad is covered by a fresh coverslip. Capillary forces are generally strong enough to hold the coverslip in place. One should avoid fixing the coverslip with nail polish as some brands of nail polish contain solvents that inhibit yeast growth.

For live imaging over longer periods of time, cells can be noncovalently immobilized on a coverslip coated with lectin and visualized in media in an observation Chamber (Ludin Chamber, Life Imaging Services, Fig. 21.2B) as described below.

1. For budding yeast, Concanavalin A (Sigma) is used at 1 mg/ml, while for fission yeast a lectin from *Neisseria gonorrhoeae* (Sigma, 1 mg/ml) is optimal. Coverslips (18 mm ø) are covered with 100 μl lectin solution which is immediately removed (the solution can be reused and kept at -20 °C).
2. Coverslips are left to dry at room temperature (>20 min) and can be kept for months protected from dust.

3. These coverslips are used in an observation chamber (Ludin chamber) that allows cells to be immersed in media that can be exchanged by continuous flow or at defined intervals (Life Imaging Services, Fig. 21.2B).
4. Cells are sedimented on the coverslip before removal of excess media. One milliliter of fresh preheated medium is then added to the cells before sealing of the chamber. If needed, a flow of medium can be used, although very slow rates (flow < 1 ml/min) should be used as pressure changes induced by liquid pumping can cause movement of the coverslips or cells in the chamber.

2.4. Controlling temperature

Stable conditions for microscopy are best achieved by temperature-controlled rooms (± 1 °C). The microscope stage itself can then be heated to the desired temperature (30 °C for wild-type strains) using a Plexiglas box that encloses the entire microscope stage (many providers now offer this option adapted to the specific instrument). Another method only heats the stage, but temperature control is less precise as an unheated objective can act as a heat sink and cool the sample during observation. Heated objectives are also available.

2.5. Image acquisition set-ups

The appropriate choice of microscope depends on the aim of the experiment. Whatever system is used, it is essential to check first that the cells survive the high-intensity light used for fluorescence illumination without damage or cell cycle arrest. The more subtle the monitored phenomenon is, the more extensive the controls must be for light-induced changes in cell physiology. The simplest assay is to compare the kinetics of cell cycle progression in cells subjected to the experimental pattern of illumination with nonimaged cells. Various time intervals, intensities of light, wavelengths and/or gray filters should be tested; unbudded cells should rebud within 120 min at room temperature after imaging on YPD.

Every microscopic system is a compromise between speed of acquisition (the higher the speed, the lower the amount of light that can be recorded), the field of acquisition (in general, the bigger the field, the slower the acquisition), and resolution (higher resolution decreases speed and signal, since each pixel on the image corresponds to a smaller part of the sample and more pixels take more time to acquire). Since the haploid yeast nucleus is only 1 μm in radius, it is recommended that the objective magnification is at least 63×, or ideally 100×, with a numerical aperture (NA) as high as possible (between 1.3 and 1.45). This allows a high-resolution camera

to obtain maximal detail from the sample (resolution power is inversely proportional to NA).

The first image acquisition setup described here is based on an improved widefield microscope, with a monochromator that regulates the light source, combined with rapid, high-precision Z motor, and a rapid and highly sensitive CCD camera for image capture. Since there is no pinhole, light from out-of-focus planes will be recorded, which can be later used by deconvolution algorithms that recalculate position of the emitted light based on an ideal or measured light spread function. The main drawback of this system is the phototoxicity due to whole cell illumination.

A second, widely available system is the laser-scanning microscope (Zeiss LSM510/710, Leica SP5). These systems have been proven very useful for acquiring very fast time-lapse recordings. Their limitation is the scanning speed, which is only fast enough for live imaging of chromatin dynamics if the field of scanning (region of interest or ROI) is reduced to a minimum (e.g., one cell). These confocals allow manual minimization of the beam intensity and pinhole. Again, there is a compromise between laser power (which increases phototoxicity, but allows more rapid image capture) and scanning speed (essential for the identification of rapid movements observed for chromatin *in vivo*).

A third system that we strongly recommend is based on a rapid, widefield high precision microscope, although the light source is a laser whose beam is focused on a rotating disk with thousands of pinholes. This disk spins at high speed dispersing the laser beam such that the whole laser power is never focused on a single point in the sample. This reduces phototoxicity and bleaching of the fluorochrome; moreover, the speed of capture is faster than that of a scanning laser system. Out-of-focus light is filtered through the pinholes, and entire fields of cells can be captured at once. In the following sections, we discuss the critical points of each of these setups.

2.5.1. Rapid high-precision widefield microscopy

For the imaging of a large number of cells at a single time point, best results are obtained with a high-precision widefield microscope. These microscopes are equipped with a piezoelectric focus either with the objective mounted on it directly (e.g., PiFoc, Physik Instrumente) or a piezoelectric table (e.g., ASI MS2000, Prior), which allows one to capture stacks of focal planes. *Z* distances between planes is carefully controlled and highly reproducible, and movement from one plane to the next is nearly instantaneous. The light source is very important, as the classical mercury bulbs show phototoxicity. The light source of choice for maximum versatility is a monochromator (Xenon light source coupled with Polychrome, TillVision), which allows excitation wavelength choice in nanometer steps (320–680 nm continuous spectrum, 20 nm window). Switching wavelengths is rapid (<1 ms). A cheaper though less flexible illumination alternative is a LED-

based illumination (CoolLED, precisExcite), where up to four wavelength (fixed) can be chosen at the time of order. LEDs are very long lived (3 years guaranteed by the supplier), which makes it a cost-effective solution. Switching time is even faster than with the monochromator (around 300 μs). From a performance point of view, we found no significant differences between a monochromator and a LED-based illumination system.

Acquisition is achieved with a high-resolution CCD camera. To detect subnuclear or subcellular details, one needs a final pixel size between 60 and 80 nm with a 100× objective. The readout of the camera by the computer is often the rate limiting factor of the system. Typically, high-speed CCD cameras (Roper Scientific Coolsnap HQ, Andor IKon, Hamamatsu ORCA) achieve about 30 frames/s, which makes exposure times shorter than 30 ms impossible. These systems are relatively inexpensive and are easier to setup than confocal microscopes. Several proprietary software can drive the entire system (microscope, camera, shutters, monochromator) such as MetaMorph (Universal Imaging).

This modified widefield microscopy is well-suited for scoring the position of a locus relative to another locus, or relative to a fixed structure (spindle pole body, nuclear periphery and nucleolus) in a large number of cells on an agarose pad. It is less well-suited for rapid, high-resolution time-lapse imaging, due to the high sampling and deconvolution that is needed for highest resolution data. If the position of two loci is to be monitored, either two different excitation colors have to be used (which increases the resolution power) or the spots have to be of significantly different sizes. 3D stacks of images are needed to evaluate the spatial positioning of the locus relative to another spot or to the nuclear periphery (see below). Optimal parameters for GFP imaging are excitation 475 nm, z-spacing 200 nm with 20 plane stacks, 100–200 ms exposure time per slice. Due to the optical resolution of the microscope, it is not useful to sample more in the z-axis, which would also increase the acquisition time, and impair accuracy if the imaged locus is moving.

For dual color imaging using CFP and YFP chromophores, optimal wavelengths are 432 and 514 nm, respectively, with exposure times of about 200 ms. The two wavelengths should be acquired successively at each focal plane. Note that the wavelengths and exposure times depend greatly on the filters present on the microscope, and should be optimized for each system (monochromators allow nm-scale changes in wavelength). A phase image is useful for determining cell cycle stage, and can be taken before or after acquisition of the fluorescence stack of images.

In widefield microscopy, an entire field of cells is illuminated during exposure. The camera records both the in-focus and out-of-focus photons. While this creates a higher background than confocal microscopy, it allows more photons to be recorded by the camera, and these signals are used for image restoration algorithms. Deconvolution is particularly powerful when

applied to widefield imaging to reassign signal to the right plane. Several software packages propose deconvolution solutions, including Metamorph, DeltaVision, and Huygens. Similarly, denoising of the images (which removes optical and electronic noise from the digitalized images) can be applied to increase the signal-to-noise ratio. Although no commercial package is available to date, development of such denoising solutions is a very active field in image processing and could lead to significant reduction of both light intensity and illumination time in the near future.

Live cell time-lapse imaging is used to record the dynamics of tagged chromatin or other subnuclear structures. Since repetitive illumination of the sample is involved, it is important to keep in mind that excitation light can stress the organism, and control experiments must be carried out to ensure that the level of illumination does not have deleterious cellular consequences. Parameters to optimize include image resolution (pixel size), the number of frames along the z-axis, excitation light intensity and exposure time.

Widefield high-precision microscopy is useful for low-frequency time-lapse imaging over fairly long periods of time (hours). The excitation light from the monochromator or the LED should be filtered using gray filters to reduce phototoxicity. Limits are set by the intensity of light used, the number of planes acquired for each time point and the time between each acquisition. In our experience, up to 300 stacks of 5 sections (1500 frames, 50 ms exposure per frame, 1 min interval between stacks) can be acquired without affecting cell cycle and with only moderate bleaching. Increasing sampling frequency will increase bleaching and damage the cells. Confocal or SD-systems are better choices for rapid time-lapse imaging, as acquisition speed is faster and photo-induced damage can be reduced by limiting the excitation time.

2.5.2. Laser-scanning microscopy

Laser-scanning systems are based on the rapid scanning of the sample by an excitation laser and recording of the emitted signal by photomultipliers (PMTs). The out-of-focus light is blocked by a pinhole which should be closed as far as possible. While these systems are well-suited to discriminate wavelengths and capture several at once, the scanning speed is often the limiting factor for image acquisition. Nonetheless, to track chromatin in individual cells at intervals of 1.5 s over timescales of 5–10 min, commercially available systems such as the Zeiss LSM510 system are well suited. This system, although slower than the newer SDs (see below), is fast enough to track significant changes in chromatin movements (jumps >0.5 μm in 10 s; Heun *et al.*, 2001b). Useful settings are described below (see also Neumann *et al.*, 2006). Note that pixel size is set by the user, and to track chromatin *in vivo* pixel size should be ≤ 100 nm. A high-resolution piezo table is essential to achieve speed and reproducibility in z position:

Laser	Argon/2 458, 488, or 514 tube current 4.7 A. Output 25%
GFP acquisition	Channel 1 LP 505 nm
YFP/CFP	Single track Channel 1 LP 530 nm Channel 3 BP 470–500 nm
Channel settings	Pinhole 1–1.2 Airy unit (optical slice 700–900 nm); detector gain 930–999; amplifier gain 1–1.5; amplifier offset 0.2–0.1 V; laser transmission AOTF 0.1–1% for GFP excitation, 1–15% for YFP, and 10–50% for CFP single track acquisition
Scan settings	Speed 10 (0.88 μs/pixel), 8 bits one scan direction; 4 average line scans; zoom 1.8 (pixel size 100 $\times$ 100 nm)
Imaging intervals	1.5 s

2.5.3. Spinning-disk confocal microscopy

As mentioned above, an attractive alternative to widefield and laser-scanning microscopes is the SD confocal. SD microscopes look similar to widefield systems yet the excitation light is provided by lasers, the beams of which are focussed on pinholes located on a disk rotating at high speed. Every point of the focal plane is illuminated several thousand times per second, but only for a fraction of a microsecond. The emitted light is filtered by passing through the pinholes to remove out-of-focus photons. Acquisition is achieved on a CCD camera, as for widefield systems. The overall quality of the picture is improved due to the confocality of the system: there is no haze as observed in widefield images. For example, nuclei which appear elongated along the *z*-axis in widefield stacks will appear more round using an SD confocal (Fig. 21.3A and B). Moreover, due to the "intermittent" excitation of fluorophores by the SD, these systems show less bleaching and phototoxicity. This allows higher frequency sampling, at a rate that is generally limited only by the acquisition rate of the camera. Where a laser-scanning confocal can record only a single nucleus with five planes and a 0.45-μm *z*-spacing, with one stack every 1.5 s, an SD system is able to record 20 planes at 0.2 μm spacing every 1.5 s, on a whole field of view.

Many systems are now available (Roper, Perkin Elmer, Andor, Zeiss provide full setups), all of which are based on Yokogawa scan heads. This head is the part which contains the SD itself, as well as filters for excitation/emission and the dichroic filter. As most of the light is stopped by the SD, powerful lasers ($>$15 mW for 488 nm excitation line) have to be used, which increases the cost of such setups. The camera can be either a classical CCD system (see above) or a more sensitive (but more noisy) EM-CCD.

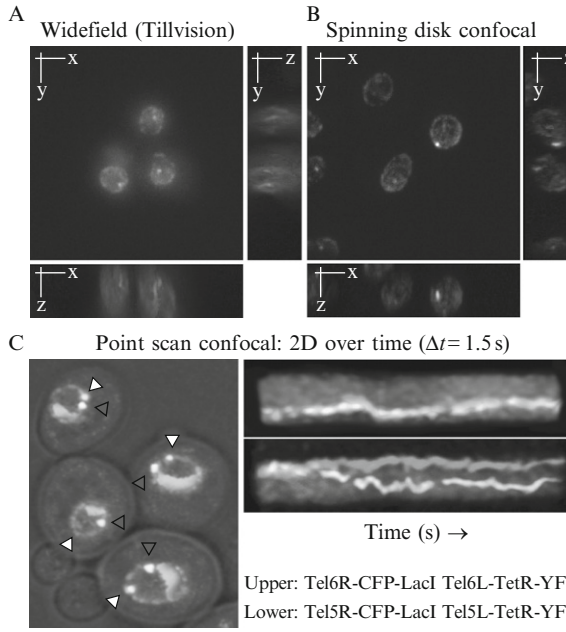

Figure 21.3 Comparison of microscope systems. (A, B) Projections in *x*–*y*, *x*–*z*, and *y*–*z* for yeast cells tagged with Nup49-GFP and a locus bearing a *lacO* array bound by a GFP-LacI fusion: (A) the image stack was taken with a high-resolution widefield microscope equipped with a monochromator and piezo (Tillvision®), while in (B) the image was taken with a spinning disk confocal. The images were not further treated or deconvolved. (C) Zeiss LSM510 confocal image of yeast cells growing in an agarose pad, bearing the following markers and fusion proteins: Nuclear envelope (Nup49-GFP, white ellipse) and the spindle pole body (Spc42-CFP, lighter spot on the nuclear envelope, indicated by a white arrow), nucleolus (Nop1-CFP, gray internal crescent), and a tagged telomere, Tel5R::*lacO* bound by GFP-LacI (gray arrow). Alongside are examples of time-lapse 2D confocal imaging on a Zeiss LSM 510 confocal microscope of two differently tagged telomeres relative to each other. They are displayed orthogonally and rotated such that the time axis (*z*) is horizontal. Top panel:Tel6L-TetR-YFP (lighter gray), Tel6R-CFP-LacI (darker gray); bottom panel (these two telomeres have been shown to colocalize (Schober *et al.*, 2009)): Tel5L-TetR-YFP (lighter gray), Tel5R-CFP-LacI (darker gray). The green background staining of the nucleus is due to the TetR-YFP diffuse in the nuclear volume (reproduced with permission from Bystricky *et al.*, 2005, see this paper for color images).

3. Data Analysis and Quantitative Measurements

3.1. Accurate determination of the 3D position of a tagged locus

To determine the position of a tagged locus inside the nucleus, the position of the center of the nucleus and of the locus have to be reconstructed from the microscopic images. As described before, the locus is usually labeled by

LacI or TetR fused to a fluorescent protein. The outline of the nucleus can be determined either by labeling a component of the nuclear pore complex or by using the background fluorescence given by unbound repressor proteins filling the nuclear volume. The latter method allows reliable identification of the center of the nucleus, yet it is difficult to measure its exact size since background fluorescence fades at the boundary. Whenever the size of the nucleus or the exact location of the NE is required, nuclear pore staining is recommended, as the boundaries of the nucleus are sharper.

The extraction of the shape of the NE and the position of a fluorescent spot from a stack of microscopic images has to deal with the anisotropy of the data, that is, the difference in optical resolution along the optical axis of the microscope (z-axis) and perpendicular to it (x/y-axes). One image (x/y-direction) has a typical optical resolution of 200 nm (with a 100× objective) and is sampled with a pixel size of 50–100 nm. In contrast, the resolution in z is not better than 300 nm even for a confocal microscope, and the images of a stack are typically taken at 200 nm steps. In addition, the fluorescent signal from the nuclear pores close to the top and bottom of the nucleus is diffuse and poorly resolved, impairing reconstruction of the NE.

We discuss here two methods to measure the position of a spot relative to the NE. Ideally, one would want to directly measure the 3D distance between the nuclear rim and the tagged locus. A budding yeast nucleus can be accurately represented by an ellipsoid or even a sphere. One possibility is therefore to fit an ellipsoid to the nuclear pore staining and use it as a model for the NE. Analogously, a 3D Gaussian distribution can be fitted to the staining of the locus to determine its position with high accuracy. The distance between the locus and the NE (or the center of the nucleus) can then be calculated using the ellipsoid and the position of the spot. However, due to the limited microscopic resolution in the z-direction ($\sim$0.6 μm for green light in widefield and $\sim$0.45 μm for a confocal), and the small size of the yeast nucleus, precise definition of the NE is particularly difficult within 0.4 μm of the top or bottom of the nuclear sphere. Attempts to solve this problem require custom-tailored multistep processing of highly sampled image stacks (Berger *et al.*, 2008), and to date no standard software has been established.

Once the position of the locus and of a second nuclear structure, such as the nucleolus or the spindle pole body, have been determined accurately, a more detailed analysis of nuclear organization can be performed based on determination of an axis within the nucleus. If only the distance of a locus to the nuclear center is measured, the nucleus is treated as spherically symmetric, which is, of course, not the case. Since the nucleolus and spindle pole body are located at opposite ends of the nucleus, they define an axis that can be exploited as a landmark for locus position. This allows one to score deviations of locus distribution from spherical symmetry (Berger *et al.*, 2008).

To deal with the poor z resolution of microscopic stacks an alternative method exploits the fact that resolution is better in x–y and a spot can be assigned to a specific plane of an image stack. Instead of calculating the 3D distance between the spot and the spherical NE directly, one measures position in the plane where the spot is brightest. In this plane, the nucleus is a circle, which can be partitioned into three concentric zones of equal area (Fig. 21.4B). The spot position is then sorted into the outermost (zone 1), the intermediate (zone 2), or the innermost zone (zone 3). To obtain equal areas for the three zones, the boundaries between zones 1 and 2 and between zones 2 and 3 are at radii of $\sqrt{2/3}R$ and $\sqrt{1/3}R$, respectively, where R is the radius of the nucleus in the chosen plane. Then it follows from the principle of Cavalieri that each zone represents one third of the nuclear volume, justifying the use of this approach.

For practical applications, we use the following procedure:

1. Measure the distance between the spot and the periphery along a nuclear diameter as well as the diameter itself. Several programs can be used to extract the coordinates of points of interest from an image. For this task, the freely available pointpicker plug-in for ImageJ is particularly useful (http://bigwww.epfl.ch/thevenaz/pointpicker/).
2. Normalize the spot pore distance to the radius (not diameter!) of the circle.
3. Sort the spot into zone 1 (if the normalized distance is $< 1 - \sqrt{2/3}$), zone 2 (if it is between $1 - \sqrt{2/3}$ and $1 - \sqrt{1/3}$), or zone 3 ($> 1 - \sqrt{1/3}$).
4. Compare the measured distribution to another one (different strain, condition, etc.) or to a uniform distribution using, for example, a χ^2 test. If only percentages of one zone (e.g., the outermost zone) are compared, a proportional test should be used.

A locus whose position is uniformly distributed will be found with an equal probability of 1/3 in each of the three zones. It should be noted, however, that the three zones do not coincide exactly with three concentric shells of equal volume, which is the desired partitioning of the nucleus, if one wishes to assess whether a locus is enriched at the nuclear periphery (Fig. 21.4D). We have calculated the error incurred by this method, and plotted it against the true distribution of spots in Fig. 21.4E. Whereas the zone measurement is no longer precise when there is strong enrichment in any of the three zones, it accurately monitors a uniform distribution of spots. Moreover, the zone method consistently underestimates enrichment or depletion, which means that any measured enrichment in one zone did not arise from an artifact of the measurement method (Gehlen, 2009).

As mentioned above, measuring spot position with respect to the NE is particularly difficult close to the poles of the nucleus. This is aggravated if the NE and spot are both tagged with GFP. To avoid severe errors that arise

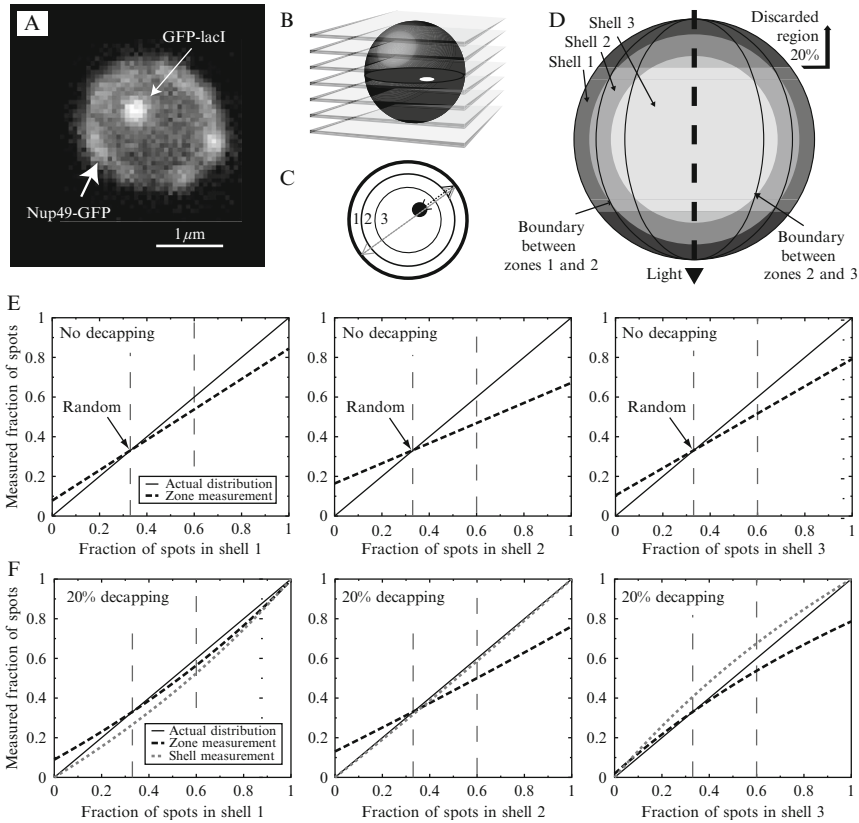

Figure 21.4 Subnuclear localization relative to the nuclear envelope: the zoning method. (A) Fluorescence microscopy image of a yeast nucleus (one plane of a 3D stack of images) bearing GFP-Nup49, a component of the nuclear pore complex, and a *lacO* array integrated into the genome and bound by a LacI-GFP fusion (fluorescent spot). (B, C) For quantification, the ring representing the nuclear envelope in the plane where the spot is brightest is partitioned into three zones of equal area. The nuclear diameter in this plane (gray arrow) and the distance of the spot to the periphery (black arrow) are measured and the ratio, which defines the localization of the spot, is scored as falling into zone 1, 2, or 3. (D) Vertical cut through the nucleus. Three shells of equal volume are shown in shades of gray. The division of the nucleus into three zones based on equal area in each plane also results in three equal volumes (the boundaries are shown as black lines), but these do not coincide exactly with shells of equal volume. Because of lack of resolution in the top and bottom slices of an image stack (see text), we remove samples in which the locus falls into the upper or lower 20% of the nuclear sphere. This so-called "decapping" is indicated in darker gray. Removal does not affect the zones and shells equally. (E) The deviation from the actual distribution in each zone when foci are scored using the zoning method with no decapping. Without decapping, the shell measurement is exact and coincides with the solid line. (F) The deviation from actual distribution is shown for foci monitored by either the zoning method or the shell method, after removal of 0.4 μm from each pole. Both types of measurements deviate from the true enrichment, although the zoning method is most accurate for zone 1. A fraction of one-third corresponds to a uniform distribution, 0.6 is a typical fraction, for example, for an anchored yeast telomere.

from such poorly resolved signals, we do not score cells in which the tagged locus is positioned within 0.4 μm of the top or bottom of the nucleus. This so-called decapping can include 3–4 planes (up to 20% of the focal planes) from each pole. While it removes questionable signals, it also affects the distribution determined by both shell (ideal 3D distance measurement) and the zoning method, because peripheral spots are more likely to be discarded than interior ones (Fig. 21.4D). In Fig. 21.4F we plot the error incurred by zoning and shell measurements as a function of spot enrichment, under decapping conditions. Intriguingly, decapping by 20% actually improves the accuracy of the zone measurements, while the shell measurements suffer from removal of these planes. Our analysis shows that the shell measurement method performs best in cases of extreme enrichment or depletion while the zoning is more accurate for moderate enrichments (35–60%), particularly in the outermost zone (zone 1). In principle, it is possible to compensate for these errors but one needs to know the exact size of the caps removed. On a practical level, it is important to remember that the zoning method accurately scores both uniformly distributed loci and distributions close to a uniform, independently of the amount of decapping performed.

3.2. Colocalization of a DNA locus with a subnuclear structure

To further investigate the function of DNA position, it is interesting to know if a fluorescently tagged locus colocalizes with other structural components of the nucleus. This can be investigated by tagging the locus in one fluorophore and the structure of interest with another, and monitoring their colocalization. Correction for chromatic shift must be made for each instrument and imaging session, by alignment of signals from small beads that emit fluorescence at multiple wavelengths.

Unless a locus is actively excluded from a subnuclear structure, a certain level of random colocalization will be detected. The amount of this background overlap will depend on the size and form of the structures monitored. To assess whether experimentally obtained colocalization values are significant or not, one must determine the expected degree of non-specific colocalization for a uniformly distributed locus. This can be calculated as the ratio between the volume of the region in which the spot is considered as colocalizing with the structure, and the total volume available to the spot.

As an example we take the binding of a chromatin locus (gene or telomere) to nuclear pores (Schober *et al.*, 2009). The diffraction limited resolution of a light microscope is not sufficient to distinguish the binding of a locus to nuclear pores from its binding to other components at the NE. A genetic trick to circumvent this problem is to examine a yeast strain with an N-terminal deletion of the nuclear pore component *NUP133* (nup133ΔN; Schober *et al.*, 2009). In this mutant the pores are not distributed all over the NE, but are clustered on one side of the nucleus

(Fig. 21.5A). A high degree of colocalization of a locus with the pore cluster may indicate specific affinity for a nuclear pore component.

To determine the colocalization arising from a uniform distribution of the locus, we first model the pore cluster as a conical disk at the nuclear periphery, whose dimensions are set based on empirical measurements. The spot is considered to colocalize with the cluster if it at least touches it (Fig. 21.5B). For the center of the chromatin spot, this defines a region that is larger than the pore cluster, which represents spot and pore colocalization. The predicted degree of background coincidence is the ratio between this colocalization volume and the total volume that is available to the spot. In the calculation of nonspecific colocalization, one can include other parameters, such as an exclusion of the spot from a subnuclear volume like the nucleolus, or a nonpore-associated enrichment at the NE. The significance of any experimental enrichment in colocalization is then determined by a proportional analysis test with a Bonferroni multiple test component.

3.3. Quantification of locus mobility

A stretch of chromatin (or any other object) inside the nucleus is exposed to numerous hits of water or other small molecules, proteins, and other macromolecules, as well as other chromatin fibers. Due to these interactions, it inevitably performs a seemingly random movement called Brownian motion. This motion is limited by the NE, but in many cases locus diffusion is even more constrained, either confined to a certain area or

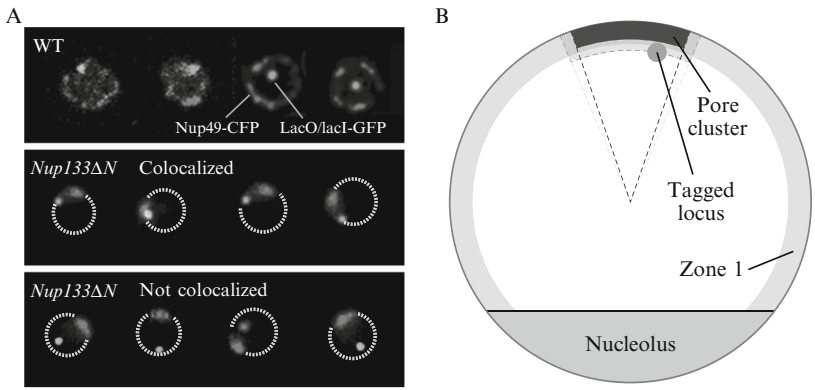

Figure 21.5 Determining the significance of colocalization. (A) Nuclear pores tagged with Nup49-GFP (red) and a LacI-tagged locus (green). The two left images in the upper panel are not deconvolved, all other images are. In the *nup133ΔN* mutant, the nuclear pores form a cluster (Schober *et al.*, 2009). (B) The expected colocalization for a randomly positioned spot and the pore cluster can be calculated as a ratio of volumes (see text). The figure shows a cut through the nucleus. The pore cluster is modeled as a conical layer shown in red. The spot is considered as colocalizing if it at least touches the pore cluster, which results in the colocalization zone (green).

obstructed by obstacles. The random movement can also be temporarily or continuously superimposed by active displacement which possibly expresses itself as increased speed and/or directionality of movement.

The first step of the quantitative analysis of chromatin movement is the determination of the position of the locus and the nuclear center for each time point of the time-lapse series. Indeed, since the nucleus itself is moving inside the cytoplasm, one must compensate for its displacement to measure the movement of a locus relative to the nucleus. Several general purpose software packages like Imaris (http://www.bitplane.com) offer object tracking functionality but usually require uniformly high-contrast images. The algorithms are mostly based on threshold principles, and it is difficult to correct insufficient results by hand. In collaboration with D. Sage and M. Unser, a dynamic programming algorithm was developed which is dedicated to the tracking of single spots in noisy images and can be applied to 2D or 3D time-lapse movies (Sage *et al.*, 2005). The algorithm is implemented as a publicly available plug-in for the free software ImageJ (http://bigwww.epfl.ch/sage/soft/spottracker/).

This tracking works in two steps: first, the images are aligned with respect to the center of the nucleus to compensate for the movement of the entire nucleus throughout the time-lapse series. A Mexican hat filter can be applied to enhance spot-like structures in the images. Next, the spot tracking is performed using three different properties of the spot:

1. *Spot intensity*: the spot fluorescence is more intense than that of the background.
2. Within one time step the spot can only travel a limited distance.
3. In contrast to nuclear pores, the spot can be located in the nuclear interior.

To reflect these properties the tracking algorithm uses four different criteria to determine the spot position at a given time point:

1. Pixel intensity
2. Displacement from the location at the previous time point
3. Displacement from the last user-defined position (see below)
4. Distance from the nuclear center

The user can give different weights to these criteria to optimize the performance of the algorithm for different situations or image qualities. Most importantly, the plug-in offers the possibility to correct the trajectory manually by forcing it to pass through a given pixel at a certain time point. The output of the plug-in is the position of spot and nuclear center for each time point.

Because of individual differences between cells it is inevitable to analyze at least 8–10 movies with a total time of more than 40 min for each strain or condition. We discuss three parameters that can be extracted from the trajectories to compare different samples.

3.3.1. Track length

A simple and robust parameter of chromatin dynamics is the track length over a time-lapse series of fixed duration. This parameter monitors average mobility of a locus and can be used for comparison of movies with the same time step and duration. It is, however, a very artificial parameter because the true trajectory of the spot is inaccessible due to the lack of temporal and spatial resolution and is much longer than the measured track length (see Fig. 21.6A for illustration).

3.3.2. Step size and large steps

The average step size of the chromatin locus within its ''walk'' is another useful characteristic. Like the track length, this parameter depends on the time step used for image acquisition, but can be used to compare differences in mobility in identically imaged samples. Directed movement does not necessarily reveal itself in large single steps but rather in several successive correlated steps. Therefore, it is also useful to look for exceptionally high displacements (''large steps'') within a certain time window. Empirically we find that a useful parameter for distinguishing patterns of mobility is the frequency of steps larger than 500 nm during 10.5 s (7 × 1.5 s steps; Heun *et al.*, 2001b).

3.3.3. Mean-squared displacement analysis

A robust method to analyze the global properties of an object's movement is the mean-squared displacement (MSD) analysis. An object in solution changes its direction when it bumps into solvent molecules and moves linearly in between, generating a random walk. If a number of objects would be initially confined in a small volume and then released, they would spread over time. It can be derived mathematically that for free diffusion the mean of the squared distance from one point on the trajectory to another is proportional to the time difference Δt: $\langle(\mathbf{r}(t+\Delta t)-\mathbf{r}(t))^2\rangle \sim \Delta t$, where $\mathbf{r}(t)$ is the position of the object at time t (Berg, 1993). The proportionality constant is usually written as $2dD$ where d is the number of dimensions and D is called the diffusion coefficient of the object. Thus, for three-dimensional free diffusion we get $\langle(\mathbf{r}(t+\Delta t)-\mathbf{r}(t))^2\rangle = 6Dt$ (Fig. 21.6).

However, in a cellular environment there is no free diffusion. The free movement of an object can be impaired by confinement, obstacles, and the binding to immobile or actively moving structures. The most inevitable restriction is the confinement of the object's movement to a nuclear or cellular compartment. This implies that the distance of any two points of the trajectory cannot exceed the maximal extension of the confining volume. Therefore, the MSD curve has to reach a plateau for large time windows (Fig. 21.6B). In the case of a spherical confinement, the value of the plateau

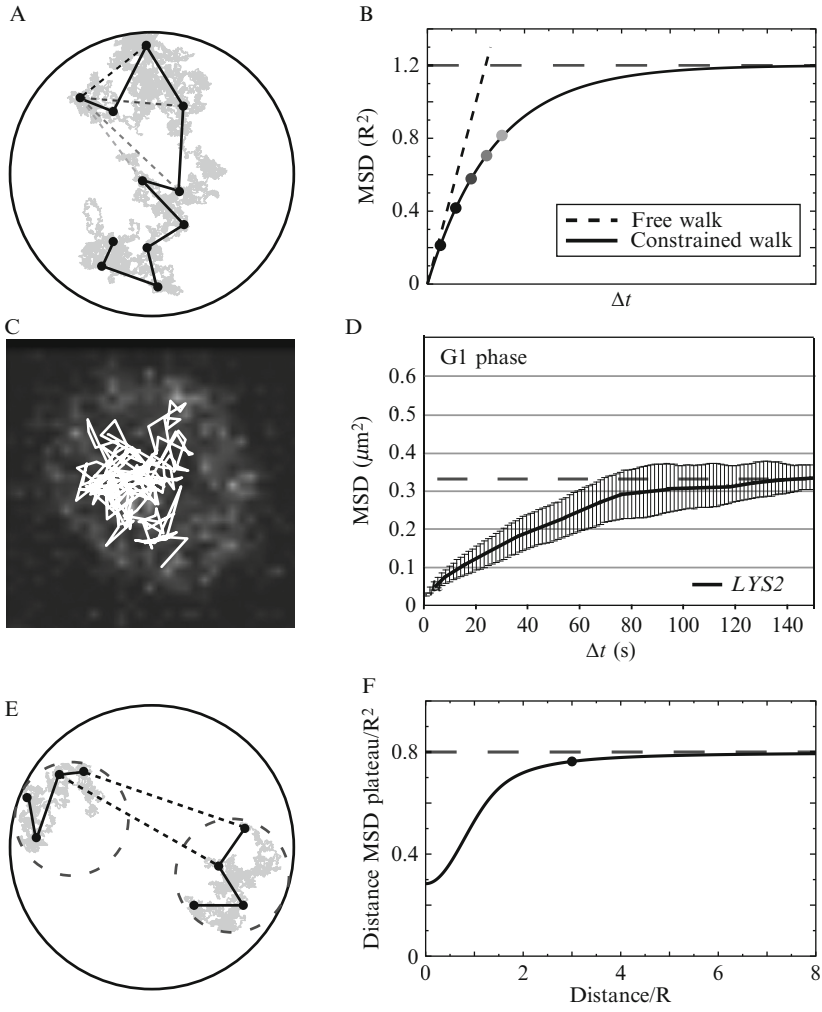

Figure 21.6 Mean-squared displacement (MSD) analysis. (A) The full trajectory of microscopic movement (light gray) cannot be detected by fluorescence microscopy due to limited resolution in time and space. A coarser trajectory (black) is recorded instead. (B) The mean of all squared spatial distances between each two points at a given time difference results in one point on the MSD graph. The mean-squared distance between a point and its successor on the trajectory is the first point on the MSD graph (black). The mean-squared distance between a point and its second successor yields the second point (dark gray) and so on. Compare the gray tones of the example distances in (A) with those of the points on the MSD graph in (B). (C) Analysis of DNA locus dynamics. The projected trace of 200 images of a movie of the *LYS2* locus is in white. The average track length in 5 min is 37.4 μm. Bar: 1 μm. (D) MSD analysis on an average of eight movies of the *LYS2* locus. All cells were observed in G1 phase. (E) The mean-squared change of spot–spot distance. In contrast to a classical MSD analysis, the mean-squared

can be calculated as $6/5R^2$, where R is the radius of the sphere (Neumann *et al.*, submitted). Thus, the so-called radius of constraint or the plateau value can be directly used as a measure for the size of the region explored by the object.

Due to the difficulties in accurately reconstructing the 3D position of fluorescent spots (see above), the movement is often observed in a 2D projection of the microscopic stacks. It can be calculated that the MSD of projected free 3D diffusion is equal to the MSD of free 2D diffusion: $\langle(\mathbf{r}(t+\Delta t)-\mathbf{r}(t))^2\rangle = 4Dt$. In the case of a spherical confinement, the MSD plateau behaves in the same way and has a value of $4/5R^2$ (see Fig. 21.6C and D; Neumann *et al.*, submitted).

For free diffusion the slope of the MSD line is a measure for the diffusion coefficient of the object, as discussed above. In the case of confined diffusion, the slope of the MSD curve is not constant. The curve is steepest at $\Delta t = 0$, and then the slope decreases monotonously (Fig. 21.6B). This is also true for diffusion with obstacles where—in the unconfined case—the MSD is not proportional to t but to t^{α} with $\alpha \neq 1$ (reviewed in Bouchaud and Georges, 1990). Nonetheless, one can still use the initial slope of the curve to compare the intrinsic mobility of different objects or one object under different conditions.

It should be noted that the movement of a locus relative to the nucleus is superimposed by the movement of the nucleus itself. Translational movement of the nucleus can be subtracted from locus movement by aligning the nuclear center throughout the time course (see Section 2.8). If two spots are observed, there is the alternative possibility to align one of the spots throughout the movie and analyze the movement of the other spot relative to the first one. This procedure also eliminates the global movement of the nucleus. However, neither the alignment of the nuclear center nor the alignment of one spot eliminates the rotational movement of the nucleus. A possibility to obtain a quantification of locus mobility that is independent of nuclear rotation is to observe the distance between the two loci and calculate the mean-squared change of this distance (see Fig. 21.6E). Since the distance between the two spots is unaffected by both translation and rotation of the nucleus, this ''distance MSD'' is only influenced by the individual movement of the two spots. The distance MSD curve shows

change of the distance between two spots instead of the mean-squared change of the position of one spot is analyzed. (F) The plateau of the distance MSD curve does not only depend on the radius of confinement R of the loci, but also on the distance d between the confining regions. However, this dependency becomes very weak for $d > 3R$. Therefore, the radius of confinement can be reconstructed from the distance MSD plateau only if the confining regions are either equal ($d = 0$) or sufficiently far from each other ($d > 3R$).

similar behavior to a classical MSD curve and has been used to derive diffusion coefficients and radii of constraints (Marshall *et al.*, 1997). However, it is important to note that the authors assumed that both loci are confined to the same region. If this is not the case, the height of the plateau, as well as the initial slope of the curve, does not only depend on the mobility of the loci but also on the distance separating the regions of constraint for the two spots. The distance MSD analysis is a valid technique to determine radius of constraint and diffusion coefficient for two diffusing spots if one of the two following conditions is fulfilled. Either (a) one can assume that the confining regions are identical (e.g., the whole nucleus) or (b) they are sufficiently far from each other. Three times the radius of constraint was found to be a reasonable threshold (Gehlen, 2009).

4. IF and FISH on Fixed Samples

Despite the power of live imaging of GFP-tagged foci, the more classical techniques of IF and FISH are recommended in several cases. First, for a scientist working alone, the analysis of multiple samples at one time point is cumbersome by live imaging. Second, if more than two DNA loci need to be imaged at once, or multiple foci in one background, FISH is more efficient. Finally, these techniques allow colocalization of protein, specific genes, and either genomic DNA or cellular substructures such as the spindle. The combination of three or four fluorochromes in a single labeling experiment is routine. Nonetheless, there are pitfalls in applying this to yeast. First, antibody background and nonspecific fluorescence signal is more often observed with yeast cells than with mammalian cells. Second, one must preserve native 3D structures of both nuclear and cytoplasmic compartments, while eliminating the cell wall to facilitate macromolecular access. To check that this was done, the integrity of an NE and the size of the nucleus can be monitored either by DNA stains or by immunolabeling with an antibody recognizing the nuclear pore (e.g., Mab414 (Abcam) which recognizes yeast Nsp1 and yields a perinuclear ring). The spherical ring structure is lost when spheroplasting conditions are too harsh or if detergent use is too high.

The diameter of an intact haploid yeast nucleus should measure between 1.8 and 2 μm, and this measurement should be monitored regularly to ensure that the nuclei observed are intact. Inappropriate methods produce flattened nuclei with a chromatin mass spanning $\sim$6–8 μm (Heun *et al.*, 2001a; Weiner and Kleckner, 1994). Due to the nature of *in situ* hybridization, accessibility of the DNA probe to the nuclear chromatin is critical and FISH protocols seek the best possible compromise between accessibility of the probe and complete integrity of nuclear and chromatin structure.

To this end, we eliminate treatments that involve protease, nuclease, and/or combinations of ionic and nonionic detergent from our protocol. We find that yeast nuclei collapse when enzymatically digested or if exposed to detergent mixtures (Gotta *et al.*, 1996; Hediger *et al.*, 2002; Heun *et al.*, 2001a). Generally, formaldehyde fixation should be performed prior to the enzymatic removal of the cell wall (spheroplasting). However, if maximal diffusion of fixative or probes is critical, spheroplasting in osmotically buffered medium can be performed prior to fixation. Double *in situ*/immunofluorescence staining often requires this type of fixation. Finally, even though cells and spheroplasts are fixed, we recommend imaging in agarose pads, since pressure on coverslips can distort 3D structure. Confocal microscopy confirms that 3D organization can be maintained by the following procedure (Heun *et al.*, 2001a).

4.1. Yeast strains and media

Diploids yeast strains may facilitate the microscopic localization of chromosomal loci, since the nuclei are nearly twice the size of haploid nuclei. There is a significant variation in the efficiency with which different strains are converted to spheroplasts, probably reflecting differences in the cell wall composition. Diploid strains usually spheroplast faster. Whenever mutants and wild type are compared we recommend using isogenic strains or strains with similar genetic background to avoid differences in the digestion time. Moreover, the efficiency of spheroplasting can be affected by growth conditions, that is, carbon source, rate of growth and stage of growth at the time of harvest. Best results are obtained with cells grown on rich medium (YPD) (Rose *et al.*, 1990) and harvested in early to mid-logarithmic phase ($0.5–1 \times 10^7$ cells/ml). When a strain background is used for the first time, it is useful to do a titration of the spheroplasting enzymes.

4.2. Antibody purification and specificity

Polyclonal antibodies can be an advantage for IF because they can recognize multiple epitopes. However, rabbit sera very often have strong background reactivity with a variety of yeast proteins, besides the desired antigen. This can be avoided in two ways: affinity purification of the specific antibodies or depletion of nonspecific antibodies by incubation with yeast deleted for the gene encoding the antigen. Affinity purification against recombinant antigen is performed as follows:

1. Transfer by Western blotting at least 50 μg of recombinant antigen to a nitrocellulose filter.
2. After staining with Ponceau red (0.05% in 3%TCA), cut out the strip containing the protein band. Wash the nitrocellulose strip 3× 10 min in

1× TEN (20 m*M* Tris–Cl, pH 7.5, 1 m*M* EDTA, 140 m*M* NaCl), 0.05% Tween 20. Block excess protein binding sites by incubating in 1× TEN + 0.05% Tween 20 + 1% dry milk powder, at room temperature for 20 min.

3. Incubate the strip with 10–50 μl of serum (depending on antibody titer and amount of antigen loaded) in 1 ml of 1× TEN, 0.05% Tween 20, 1% dry milk powder, overnight at 4 °C with constant agitation (rocker or wheel).
4. Remove the supernatant, wash the strip 3× 10 min in 1× TEN, 0.05% Tween 20 at room temperature. Elute the bound immunoglobulin with 300 μl of cold 0.1 *M* glycine, pH 3.0, for 2 min.
5. Immediately raise the pH to 7.0 by adding 1 *M* Tris base (the volume required should be determined empirically before starting), and place on ice.
6. Repeat the elution once or twice and pool the elutions that contain antibody. Note that it may be necessary to drop the pH of the glycine to pH 1.9 for efficient elution.
7. The antibodies can be stored as aliquots at −80 °C. Stabilization is enhanced by addition of 1–2% ovalbumin and 20% glycerol. The antibody is used at a dilution of 1:2 or more for IF. The specificity of the purified antibodies should be demonstrated by Western blot and IF on strains lacking the protein in question.

If recombinant antigen is not available, rabbit sera can be preadsorbed against fixed yeast spheroplasts from a strain lacking the desired antigen. Incubation of antiserum and cells can be performed for several hours, and the nonbound antibodies are used on the test sample after sedimentation of the fixed spheroplasts.

Monoclonal antibodies usually recognize a single epitope which reduces background in yeast, yet some commonly used monoclonals (e.g., anti-HA) do recognize an endogenous yeast protein epitope. This can be tested on Western blots, although SDS denatured antigens are not always equivalent to formaldehyde fixed ones. The obvious disadvantage of staining for a unique epitope is that the risk is greater that it is masked or denatured by the fixation conditions.

The fluorophore-coupled secondary antibodies should always be tested on permeabilized material lacking the primary antibody to assess the background fluorescence created by unspecific binding of the secondary antibodies. To improve signal specificity it is advisable to preabsorb the secondary antibody on fixed yeast cells, and to dilute it maximally to avoid unnecessary background.

4.3. Choice of fluorophores

For efficient visualization of several targets, fluorophores should be chosen that are excited and visualized independently. This depends on the excitation lines and filter sets available in your microscope. If there is overlap between

the emission spectra, we recommend attenuating some signals by controlling the intensity of the excitation line (e.g., on a confocal microscope) to avoid "bleed through." Some of the more commonly used fluorophores are Alexa Fluor conjugated antibodies at several excitation/emission wavelengths (Molecular Probes, Invitrogen), Cy3 ($A = 554$ nm, $E = 566$ nm) and Cy5 ($A = 649$ nm, $E = 666$ nm). The Alexa fluorophores offer the advantage of increased photostability, as compared to the older Cy dyes.

4.4. Protocol

We present here one protocol for combined IF/FISH, but the same procedure can be used to perform only IF by omitting Sections E and F, or only FISH by omitting Section D. Follow all Sections A–G for combined IF/FISH.

(A) Fixation

Cells are fixed either before or after conversion to spheroplasts by the addition of freshly dissolved paraformaldehyde (not glutaraldehyde). If preservation of cell shape and cytosolic structures is required, then cells should be fixed before spheroplasting. For detection of low abundance nuclear antigens, postspheroplasting fixation can be used. A fresh stock solution of 20% paraformaldehyde should be prepared before the experiment begins by mixing 5 g of paraformaldehyde, 15 ml H_2O and 25 μl 10 N NaOH. Dissolve at 70 °C in a closed bottle in a fume hood for about 30 min with occasional shaking. Adjust final volume to 25 ml and cool on ice. Note that paraformaldehyde fumes are toxic and care should be taken with this reagent. The commercially available 37% formaldehyde solution, while less toxic, has long formaldehyde polymers that hinder entry into cells. Glutaraldehyde should be avoided since it often masks or destroys antigenic epitopes.

1. Grow yeast cells overnight to about 1×10^7 cells/ml in 50 ml YPD or selective media (Rose *et al.*, 1990).
2. Adjust to 4% paraformaldehyde (final concentration) and incubate 15 min at room temperature. For a 20-ml culture one would add 5 ml of 20% paraformaldehyde. If fixation is performed in synthetic medium, the fixative should be quenched by adjusting to 0.25 *M* glycine or 0.1 *M* Tris–Cl, pH 8.0, after 15 min.
3. Centrifuge 5 min at 800×*g*.
4. Carefully resuspend the pellet in 40 ml of YPD and centrifuge 3 min at 800×*g*.
5. Repeat step 4.

Resuspend pellet in YPD (1/10 of initial culture volume) and keep it at 4 °C (up to overnight) or proceed to spheroplasting using the

protocol below. If epitopes are of low abundance, it may be preferred to spheroplast prior to fixation. In this case start with Section B.

(B) Spheroplasting

6. Harvest cells at 1200×*g* for 5 min at room temperature in preweighed 50 ml polypropylene tubes.
7. Decant the supernatant and weigh the cell pellet.
8. Resuspend the cells in 1 ml/0.1 g of cells 0.1 *M* EDTA–KOH (pH 8.0), 10 m*M* DTT. DTT has to be added freshly. Use roughly 1/20 culture volume of EDTA–DTT solution.
9. Incubate at 30 °C for 10 min with gentle agitation.
10. Collect the cells by centrifugation at 800×*g* for 5 min at room temperature.
11. Carefully resuspend the cell pellet in 1 ml/0.1 g cells YPD + 1.2 *M* sorbitol (mix 22 g sorbitol with 100 ml YPD). To resuspend evenly, suspend the cell pellet first in 500 μl.
12. Add lyticase (β-glucanase; Verdier *et al.*, 1990) to 250–500 U/ml and predissolved Zymolyase (20T, Seikagaku) to final 10–100 μg/ml. This step is critical; appropriate amounts of enzyme should be determined in a trial experiment with the same cells.

For a 20-ml culture we use 2 ml of solution with 12 μl lyticase (40,000 U/ml) and 4 μl of Zymolyase (20T) freshly dissolved in YPD at 5 mg/ml. Because diploid strains spheroplast faster than haploid strains, we often pretreat with only 1 m*M* DTT and use half of the final concentration of lyticase and Zymolyase for diploid cells.

13. Incubate at 30 °C in the original Erlenmeyer flask with gentle agitation (150 rpm) and monitor spheroplast formation in the microscope at 5, 10, 15, and 20 min.

The appropriate stage of spheroplasting is determined by microscopic observation with polarized light. Initially cells will have a bright interior and a bright halo. Well spheroplasted cells become dark with a bright halo around the cell shape. When cells are dark inside and do not have the bright halo outside anymore, spheroplasting has been carried out for too long. This leads to a loss of antigen by diffusion and an altered 3D structure of the cell. In a given culture, speed of spheroplasting varies among cell stages, thus it is therefore advisable to stop digestion when 50% of the cells are properly spheroplasted.

14. Dilute with YPD + 1.2 *M* sorbitol to 40 ml. Centrifuge 5 min at 800×*g*.
15. Wash twice in 40 ml YPD + 1.2 *M* sorbitol, resuspending gently using a rubber bulb on the end of pipette (do not vortex or use glass rods). Centrifuge 5 min at 800×*g*.

If cells were not fixed prior to spheroplasting, resuspend the spheroplasts gently in 0.5× culture volume of YPD + 1.2 *M* sorbitol, and fix by incubating at room temperature in 4% paraformaldehyde (final

concentration) for 15 min. All washes should be done with YPD + 1.2 *M* sorbitol to avoid cell lysis.

(C) Cell permeabilization

16. Resuspend fixed spheroplasts thoroughly in YPD + 1.2 *M* sorbitol (0.5 g in 0.8 ml). Sorbitol can be omitted for cells that were fixed first prior to spheroplasting. The concentration of cells in this suspension should be such that only one layer of nonconfluent cells will adhere to the slide. Leave a drop on each spot of Teflon-coated slides (Super-Teflon slides, Milian) for 1–2 min to allow adherence, and remove as much liquid as possible using a pipet. Superficially air dry 2 min. All the following washes are performed by immersing the slide in a Coplin jar containing the indicated solution.
17. Place the slides in prechilled methanol at −20 °C for 6 min.
18. Transfer the slides to prechilled acetone at −20 °C for 30 s.
19. Air dry 3 min.

(D) Antibody treatment (IF)

20. Incubate slides in 1× PBS (Sambrook *et al.*, 1989) + 1% ovalbumin + 0.1% Triton X-100 for 20 min or more. Shake gently two or three times at room temperature. After this step the cells appear transparent and nuclei can be seen as a dark spot. This is an indication of good spheroplasting. If this is not the case, it may help to leave the slides for up to an hour in PBS + 1% ovalbumin + 0.1% Triton X-100.
21. Dry the Teflon surfaces and bottom of the slides with a paper tissue.
22. Cover each spot on the slide with 25 μl of the appropriate primary antibody diluted as required in PBS containing 0.1% Triton X-100. For affinity purified antibodies start with a 1/20 dilution in 0.5× PBS + 0.1% Triton X-100 to avoid high salt concentrations. For overnight incubation Triton should be avoided.
23. Incubate for 1 h at 37 °C in a humid chamber or overnight at 4 °C. In the latter case the slides should be covered with a coverslip (but not sealed) to avoid drying of the antibody solution.
24. Preabsorb the secondary antibody on yeast cells. For this purpose, use the remaining fixed spheroplasts by washing them 3× in PBS containing 0.1% Triton X-100 and resuspending them in 1 ml of PBS. Dilute the secondary antibody (stock is usually 1 mg/ml) 1:250 in this spheroplast suspension and incubate for 30 min on a rotating wheel at 4 °C in the dark. Centrifuge at top speed. Store on ice until needed.
25. After the primary antibody incubation, wash the slides 3× 5 min by immersion in PBS + 0.1% Triton X-100 in a Coplin jar at room temperature.

26. Dry the Teflon surfaces and bottom of the slides. Cover each slide with 25 μl/spot of the fluorescent secondary antibody after preadsorption and incubate for 1 h either at room temperature or 37 °C in a dark, humid chamber.
27. After the secondary antibody, wash the slides 3× 5 min in PBS + 0.1% Triton at room temperature.

(E) *In situ* hybridization probes

To label probes for FISH, plasmids containing the target sequence can be used as well as PCR fragments amplified using appropriate primers. For optimal FISH signals a fragment of 6–10 kb from a genomic locus should be used as a template for nick-translation to prepare probes. Fragments as small as 2 kb can be used, although labeling efficiency will be lower. Final probe length should be between 200 and 300 nucleotides after nick-translation. This can be checked by running the final probe on a 2% agarose gel. Probes for FISH are labeled by a nick-translation protocol for which kits are commercially available (e.g., Nick Translation Mix, Roche). The fluorescent labeling can be carried out either during the nick-translation reaction or indirectly using an antibody against modified nucleotides. Detailed protocols for probe preparation have been published previously (Gotta *et al.*, 1999; Heun *et al.*, 2001a).

Direct labeling of the probe is achieved by using a fluorescently labeled dUTP (Alexa fluor dUTP, Invitrogen) in place of dTTP in the nick-translation reaction. Efficiency of the Alexa-dUTP incorporation into the probe can be quantified using a Fluorimeter (NanoDrop), or the fluorescence in the dried probe pellet can be directly visualized under a fluorescent microscope. Alternatively, commercially available kits offer a two-step labeling using amine-modified dUTP, which will then be cross-linked to fluorochromes (FISH-Tag, Invitrogen). Since the amine modification is small compared to Alexa molecules, the nick-translation reaction is more efficient and the resulting probe is brighter. Finally, probe labeling can also be achieved using digoxigenin-derivatized dUTP (dig-dUTP, Roche). Note that the detection of the digoxigenin-derivatized dUTP will require an antidigoxigenin fluorescent primary antibody or an antidigoxigenin primary antibody and a fluorescently labeled secondary antibody. This approach can be used to amplify weak signals.

(F) FISH

If only FISH is to be performed go directly from step 19 (cell permeabilization) to step 30. For a combined IF/FISH protocol continue here with step 28, which prevents primary or secondary antibody dissociation under the harsh conditions used for FISH

28. Postfix the cells in 4× SSC, 4% paraformaldehyde 20 min at room temperature after the last wash. Rinse 3× 3 min in 4× SSC.
29. Immerse cells in 4× SSC, 0.1% Tween 20, 20 μg/ml preboiled RNaseA (optional). Incubate overnight at room temperature (in the dark if IF was performed).
30. Wash in H_2O.
31. Dehydrate in ethanol: 70%, 80%, 90%, and 100% consecutively at −20 °C, 1 min each bath.
32. Air dry.
33. Add 10 μl/spot of 2× SSC, 70% formamide. Cover with a coverslip. Leave 5 min at 72 °C (place the slide on top of an aluminum block which is partially submerged in a 72 °C waterbath. On the narrow edges of the slide, place few drops of water, which will spread between the aluminum block and the slide, improving the heat conductance).
34. Dehydrate in ethanol: 70%, 80%, 90%, and 100% consecutively at −20 °C, 1 min/bath.
35. Air dry.
36. Apply hybridization solution, 3 μl for each spot. The optimal concentration of probe depends on the sequence and must be determined empirically. Place a coverslip on top avoiding air bubbles, seal with nail polish.
37. Incubate 10 min at 72 °C.
38. Incubate 24–60 h at 37 °C.
39. Remove the coverslip and wash twice in 0.05× SSC, 5 min at 40 °C.
40. Incubate in BT buffer (0.15 *M* $NaHCO_3$, 0.1% Tween 20, pH 7.5) 0.05% BSA, 2× 30 min at 37 °C in the dark.
41. If FISH probe was labeled using digoxigenin-derivatized dUTP continue with step 42.

If probe was done using a fluorescent dUTP go directly to visualization or stain DNA by following step 45.

42. Add mouse antidigoxigenin diluted 1:50 in BT buffer without BSA + the secondary goat–anti-mouse or rabbit antibody 1:50 (for refreshing the IF signal, if necessary; Boehringer Mannheim). Stock solutions are usually 1 mg/ml. At this point you can either use derivatized sheep anti-Dig (rhodamine or FITC derivatized) or detect the protein two steps, first with a nonderivatized primary mouse–anti-DIG, and then with a secondary fluorescent antibody to amplify the anti-DIG signal. For two-step labeling, repeat steps 42–44 twice.
43. Incubate 1 h at 37 °C in a humid chamber.
44. Wash 5× 3 min in BT buffer.

(G) DNA visualization

To visualize DNA, you must avoid the wavelengths of excitation and emission relevant for the fluorophores used. The most frequent staining agents used are ethidium bromide (diluted to 1 μg/ml in antifade reagent excitation 518 nm/emission 605 nm), DAPI (1 μg/ml, excitation 358 nm/emission 461 nm), or cyanine nucleic acid dyes (TOTO/POPO/YOYO/BOBO family of dyes, Molecular Probes).

45. Add 25 μl/spot of the DNA stain agent diluted in 1× PBS + 0.1% Triton X-100 for 10min at room temperature.
46. Wash in 1× PBS + 0.1% Triton X-100.
47. Dry the black Teflon surface and bottom of the slides and add one drop of antifade solution (Prolong antifade, Invitrogen). An alternative antifade is 1× PBS, 50% glycerol, 24 μg diazabicyclo-2,2,2-octane or DABCO, pH 7.5.
48. Cover with a coverslip avoiding air bubbles. Slides can be examined immediately or kept at 4 °C in the dark overnight. For longer storage, seal the coverslip with nail polish and keep at 4 °C in the dark or at −80 °C.

4.5. Special notes

To monitor different targets at a time, primary antibodies from different species must be used (e.g., mouse, rabbit, sheep) and species-specific secondary antibodies. To reduce incubation times, we recommend mixing primary or secondary antibodies. However, it is essential to pretest the secondary antibody with each of the primary antibodies separately to ensure that they do not cross react.

An alternative way to localize proteins both in living and in fixed cells is to generate a GFP fusion (Shaw *et al.*, 1997), although proteins fused to GFP must be tested for proper functionality. When the GFP-fluorescence signal is very strong (abundant or overexpressed proteins), it can sometimes be visualized after the IF protocol. For weaker signals, or CFP fusions, samples should be fixed with 1% paraformaldehyde for 3 min and washed at least three times with 1× PBS. These samples need to be visualized by microscopy as quickly as possible. Epifluorescence (particularly for CFP) will not last long than a week at 4 °C. For visualization of a strong GFP signal cells can also be fixed with ethanol 80% for 5 min and washed with 1× PBS containing DAPI. Alternatively GFP fusions can be detected using the IF protocol and anti-GFP antibodies.

It is not always necessary to preserve 3D nuclear structure, for example, for scoring mitotic or meiotic chromosome pairing (Guacci *et al.*, 1994; Weiner and Kleckner, 1994). However, one must be careful not to draw conclusions about nuclear architecture from results obtained with flattened or spread preparations.

For time-course experiments, or when a large number of samples need to be handled (20 or more), we recommend to fixing overnight at 4 °C, and performing spheroplasting the next day. For unexplained reasons, one uses half the amount of lyticase and Zymolyase under these circumstances. Moreover, spheroplasts can be spotted on glass, permeabilized and kept at 4 °C in blocking solution without Triton X-100 for extended periods of time. Prolonged exposure to Triton X-100 should be avoided. Some protocols recommend coating slides with poly-lysine (Sigma, P8920) to promote spheroplast or cell attachment, but we avoid it because it increases background fluorescence. Plastic multiwell slides (μ-Slide, Ibidi) can be used to spot multiple samples on one slide, reducing the number of slides needed.

This protocol is not only useful for *S. cerevisiae*, but has also been successfully used for *Neurospora crassa*. We used Novozyme 234 (Novo Biolabs) instead of Zymolyase to digest the *Neurospora* cell wall, and incubation times with the antibodies tested were increased to 48 h.

REFERENCES

Belmont, A. S. (2001). Visualizing chromosome dynamics with GFP. *Trends Cell Biol.* **11,** 250–257.

Berg, H. C. (1993). *Random Walks in Biology*. Princeton University Press, Princeton, NJ.

Berger, A. B., Cabal, G. G., Fabre, E., Duong, T., Buc, H., Nehrbass, U., Olivo-Marin, J. C., Gadal, O., and Zimmer, C. (2008). High-resolution statistical mapping reveals gene territories in live yeast. *Nat. Methods* **5,** 1031–1037.

Bouchaud, J.-P., and Georges, A. (1990). Anomalous diffusion in disordered media: Statistical mechanisms, models and physical applications. *Phys. Rep.* **195,** 127–293.

Bressan, D. A., Vazquez, J., and Haber, J. E. (2004). Mating type-dependent constraints on the mobility of the left arm of yeast chromosome III. *J. Cell Biol.* **164,** 361–371.

Bystricky, K., Laroche, T., van Houwe, G., Blaszczyk, M., and Gasser, S. M. (2005). Chromosome looping in yeast: Telomere pairing and coordinated movement reflect anchoring efficiency and territorial organization. *J. Cell Biol.* **168,** 375–387.

Gehlen, L. R. (2009). *Biophysical analysis of diffusion controlled processes in the budding yeast nucleus*. PhD thesis, University of Basel.

Gotta, M., Laroche, T., Formenton, A., Maillet, L., Scherthan, H., and Gasser, S. M. (1996). The clustering of telomeres and colocalization with Rap1, Sir3, and Sir4 proteins in wild-type Saccharomyces cerevisiae. *J. Cell Biol.* **134,** 1349–1363.

Gotta, M., Laroche, T., and Gasser, S. M. (1999). Analysis of nuclear organization in Saccharomyces cerevisiae. *Methods Enzymol.* **304,** 663–672.

Guacci, V., Hogan, E., and Koshland, D. (1994). Chromosome condensation and sister chromatid pairing in budding yeast. *J. Cell Biol.* **125,** 517–530.

Hediger, F., Dubrana, K., and Gasser, S. M. (2002). Myosin-like proteins 1 and 2 are not required for silencing or telomere anchoring, but act in the Tel1 pathway of telomere length control. *J. Struct. Biol.* **140,** 79–91.

Hediger, F., Taddei, A., Neumann, F. R., and Gasser, S. M. (2004). Methods for visualizing chromatin dynamics in living yeast. *Methods Enzymol.* **375,** 345.

Heun, P., Laroche, T., Raghuraman, M. K., and Gasser, S. M. (2001a). The positioning and dynamics of origins of replication in the budding yeast nucleus. *J. Cell Biol.* **152,** 385–400.

Heun, P., Laroche, T., Shimada, K., Furrer, P., and Gasser, S. M. (2001b). Chromosome dynamics in the yeast interphase nucleus. *Science* **294,** 2181–2186.

Hom, E. F., Marchis, F., Lee, T. K., Haase, S., Agard, D. A., and Sedat, J. W. (2007). AIDA: An adaptive image deconvolution algorithm with application to multi-frame and three-dimensional data. *J. Opt. Soc. Am. A Opt. Image Sci. Vis.* **24,** 1580–1600.

Kitamura, E., Blow, J. J., and Tanaka, T. U. (2006). Live-cell imaging reveals replication of individual replicons in eukaryotic replication factories. *Cell* **125,** 1297–1308.

Lisby, M., Mortensen, U. H., and Rothstein, R. (2003). Colocalization of multiple DNA double-strand breaks at a single Rad52 repair centre. *Nat. Cell Biol.* **5,** 572–577.

Marshall, W. F., Straight, A., Marko, J. F., Swedlow, J., Dernburg, A., Belmont, A., Murray, A. W., Agard, D. A., and Sedat, J. W. (1997). Interphase chromosomes undergo constrained diffusional motion in living cells. *Curr. Biol.* **7,** 930–939.

Michaelis, C., Ciosk, R., and Nasmyth, K. (1997). Cohesins: Chromosomal proteins that prevent premature separation of sister chromatids. *Cell* **91,** 35–45.

Neumann, F. R., Hediger, F., Taddei, A., and Gasser, S. M. (2006). Tracking individual chromosomes with integrated arrays of lac^{op} sites and GFP-lacI repressor: Analysing position and dynamics of chromosomal loci in *Saccharomyces cerevisiae*. *In* ''Cell Biology A Laboratory Handbook.'' (J. E. Celis, ed.), Vol. 2, pp. 359–367. Elsevier Science.

Neumann, F. R., Dion, V., Gehlen, L. R., Tsai-Pflugfelder, M., Taddei, A., and Gasser, S. M. INO80 promotes chromatin movement and functionally impacts homologous recombination. submitted.

Rohner, S., Gasser, S. M., and Meister, P. (2008). Modules for cloning-free chromatin tagging in Saccharomyces cerevisiae. *Yeast* **25,** 235–239.

Rose, M. D., Winston, F., and Hieter, P. (1990). Methods in Yeast Genetics. Cold Spring Harbor Laboratory Press, New York.

Sage, D., Neumann, F. R., Hediger, F., Gasser, S. M., and Unser, M. (2005). Automatic tracking of individual fluorescence particles: Application to the study of chromosome dynamics. *IEEE Trans. Image Process.* **14,** 1372–1383.

Sambrook, J., Fritsch, E. F., and Maniatis, T. (1989). *Molecular Cloning: A Laboratory Manual* 2nd ed. Cold Spring Harbor Laboratory Press, Cold Spring Harbor, NY.

Schober, H., Ferreira, H., Kalck, V., Gehlen, L. R., and Gasser, S. M. (2009). Yeast telomerase and the SUN domain protein Mps3 anchor telomeres and repress subtelomeric recombination. *Genes Dev.* **23,** 928–938.

Shaw, S. L., Yeh, E., Bloom, K., and Salmon, E. D. (1997). Imaging green fluorescent protein fusion proteins in Saccharomyces cerevisiae. *Curr. Biol.* **7,** 701–704.

Straight, A. F., Belmont, A. S., Robinett, C. C., and Murray, A. W. (1996). GFP tagging of budding yeast chromosomes reveals that protein-protein interactions can mediate sister chromatid cohesion. *Curr. Biol.* **6,** 1599–1608.

Taddei, A., Hediger, F., Neumann, F. R., Bauer, C., and Gasser, S. M. (2004). Separation of silencing from perinuclear anchoring functions in yeast Ku80, Sir4 and Esc1 proteins. *EMBO J.* **23,** 1301–1312.

Verdier, J. M., Stalder, R., Roberge, M., Amati, B., Sentenac, A., and Gasser, S. M. (1990). Preparation and characterization of yeast nuclear extracts for efficient RNA polymerase B (II)-dependent transcription in vitro. *Nucleic Acids Res.* **18,** 7033–7039.

Weiner, B. M., and Kleckner, N. (1994). Chromosome pairing via multiple interstitial interactions before and during meiosis in yeast. *Cell* **77,** 977–991.